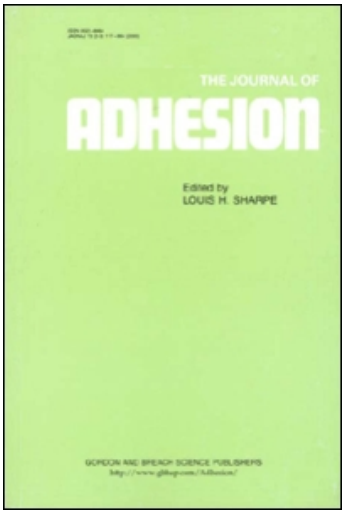

The Journal of Adhesion
Publication details, including instructions for authors and subscription information:
http://www.informaworld.com/smpp/title~content=t713453635

Influence of Matrix Properties on Fragmentation Test

J. P. Armistead[a]; A. W. Snow[a]
[a] U. S. Naval Research Laboratory, Materials Chemistry Branch, Washington D. C., USA

To cite this Article Armistead, J. P. and Snow, A. W.(1995) 'Influence of Matrix Properties on Fragmentation Test', The Journal of Adhesion, 52: 1, 209 — 222
To link to this Article: DOI: 10.1080/00218469508015194
URL: http://dx.doi.org/10.1080/00218469508015194

J. Adhesion, 1995, Vol. 52, pp. 209–222
Reprints available directly from the publisher
Photocopying permitted by license only

Influence of Matrix Properties on Fragmentation Test*

J. P. ARMISTEAD and A. W. SNOW

U. S. Naval Research Laboratory, Materials Chemistry Branch, Washington D. C. 20375, USA

(*Received March 14, 1994; in final form August 26, 1994*)

Physical aging was used to vary the mechanical properties of model single fiber composites without changing the chemistry at the interface in order to study how property changes affect the measurement of interfacial adhesion by the fragmentation test. The properties of epoxy matrix/AS4 single fiber composites driven to full cure ($T_g = 166°C$) are altered by annealing below T_g. Neat resin samples with identical thermal histories are tested. All aged panels show roughly the same embrittlement with aging characterized by an average 30% decrease in tensile failure strain and 7.3% increase in compressive yield relative to quenched samples. Fragmentation results indicated no change between aged and quenched samples. Results are discussed in terms of micromechanics models for the fragmentation test. Strain at fragmentation increased with aging. This was related to the residual stress state in the model composite and the possibility of the zero stress state of the single fiber composites increasing with thermal annealing.

KEY WORDS fragmentation test; composites; fiber/matrix interface; fiber/matrix adhesion; carbon fibers; epoxy resin; mechanical properties; physical aging

1. INTRODUCTION

The single fiber fragmentation test has received a lot of attention both as a diagnostic for fiber/matrix adhesion and as a simple composite system amenable to micromechanics modelling. The test has been shown to have high sensitivity relative to other microscale adhesion tests[1] and measured adhesion changes correlate well with macroscopic composite properties.[2] One problem with the fragmentation test is that there is currently no accepted way to obtain absolute interfacial adhesive parameter (s) from the measured data although many micromechanics models exist.This is because of the complexity of the interface and a multitude of failure modes (each requiring a different treatment). Evaluation of models is difficult because as matrix property changes are made to test the models, there can be unwanted (and undefined) changes in interfacial chemistry and /or changes in interface failure mode. In this study, we minimize the possibility of interfacial chemistry changes by using physical aging to induce small changes in matrix properties. Resultant changes in the fragmentation results are compared with aging-induced bulk properties to evaluate the models.

* Presented at the Seventeenth Annual Meeting of The Adhesion Society, Inc, in Orlando, Florida, U.S.A., February 21–23, 1994. One of a Collection of papers honoring Lawrence T. Drazal, the recipient in February 1994 of *The Adhesion Society Award for Excellence in Adhesion Science, Sponsored by 3M.*

2. BACKGROUND: FRAGMENTATION TEST, INTERFACIAL FAILURE MODES

Study of the interface in composites is like any other adhesion problem in that it involves physical origins such as fiber geometry and surface roughness, mechanical origins such as cure and Poisson stresses, and chemical origins which could be anything from van der Waals forces to covalent bonds. In a series of papers by Drzal and coworkers, the usefulness of the single fiber fragmentation test was illustrated for carbon fiber/epoxy matrix composites.[2-6] In this test, a single fiber is mounted along the axis of a tensile coupon of matrix resin. The tensile coupon is strained while under observation in a polarizing microscope. As the tensile coupon is strained the fiber fragments, owing to loading through shear stresses at the fiber/matrix interface. Fragmentation stops when all fragments are shorter than the "critical length", which is the length necessary to develop tensile stresses in the fragment which are greater than the fiber strength at that gauge length. The fragment length distribution is measured and is used to estimate the adhesion at the interface. An added benefit of this technique is the birefringence patterns that appear in the matrix, accompanying the fragmentation process, which are useful in ascertaining the interfacial failure mode.

Using the fragmentation test, Drzal and coworkers found that commercial oxidation processes remove an outer weak layer in high strength fibers allowing good adhesion to occur. High modulus fibers adhere poorly to matrix resins probably due to the morphological nature of the fiber surface, and adhesion improves with the number of oxygen-containing groups on the fiber surface. The birefringence patterns result from the propagation of a crack along the interface emanating from fragmentation events. Two distinct cases were noted: good adhesion in which there is a lot of matrix plastic deformation accompanying the crack propagation and poor adhesion in which there is very little plastic deformation.[3]

Since this work, the fragmentation test has become a widely used technique for carbon fiber/organic matrix systems because it is relatively simple and the results are sensitive and reproducible. Further work has shown that the adhesion improvements seen in fragmentation testing correlate with improvements in composite properties.[2] A recent round-robin study[1] confirmed the sensitivity of the technique, but also pointed out lab-to-lab variations in the results and the fact that there is still no single accepted technique for relating the measured fragment distribution to the adhesion at the interface. The reasons for this lie not only in the chemical and physical adhesive forces at the interface, but also in the geometry and residual stress state of the test specimen, the nonlinear viscoelastic nature of many matrix resins, the gage length dependence of the fiber tensile strength and, in a multitude of failure (fragmentation) mechanisms. No one model will describe all fragmentation modes, and evaluation is difficult when the pertinent variables are not independent and attempting to alter them may unwittingly change the interfacial adhesion.

Many investigators calculate a shear stress parameter (τ) from the measured fragment lengths using the equation derived by Kelly and Tyson for a brittle fiber in a ductile matrix.[7]

$$\tau = (\sigma_f d)/(2l_c) \tag{1}$$

In the above equation, d is the fiber diameter, σ_f is the fiber failure stress at the critical fragment length, and l_c is the critical fragment length. Though the equation appears simple, carbon fibers are brittle and fail at inherent flaws. This makes the fiber failure stress gauge-length-dependent and also results in a statistical distribution of fragment lengths. Techniques for handling the distribution of fragments vary from simply using average critical lengths and failure stresses to incorporating statistically, each fragmentation event.[1,8,9] Though no matrix properties are used in the calculation of τ, the model is based on plastic deformation of the matrix resin and a uniform stress transfer along the length of the fragments. When there is good adhesion, the measured adhesion would approach, and be limited by, the shear strength of the resin near the interface.

Investigators have also proposed to approximate the matrix behavior as elastic.[10,11] Most of these models are similar to, or based on, the shear-lag analysis of Cox.[12] For this model, the interfacial shear strength, ISS, is dependent on the matrix strain, ε_m, the matrix shear modulus, G_m, and E_f, the fiber modulus, as shown below.

$$\tau = const\, \varepsilon_m (G_m E_f)^{0.5} \tag{2}$$

These models have been evaluated by altering matrix properties with chemistry or temperature changes while assuming constant interfacial adhesion.[10,13–15] In general, increases in fragment lengths were observed for lower matrix modulus and shear strength, as expected, but neither model fit convincingly. This may be because the models are oversimplified for the complexity of the test. Other factors include changes in failure modes due to large property changes (testing above and below T_g) or that chemistry changes actually altered the interfacial adhesion.

The birefringence patterns and measured ISS values reflect distinct failure modes in the fragmentation test. Drzal and coworkers showed that the matrix deformation illustrated by the birefringence is often the result of propagation of a crack along the interface.[4] The above models do not take this into consideration and may only be realistic when very little crack propagation occurs (or if it occurs, it happens at high matrix strains long after fragmentation has ceased). There are at least three distinct types of birefringence patterns for thermoset/carbon fiber systems. The first is characterized by low ISS values, long crack propagation lengths, and faint birefringence patterns with very little matrix plastic deformation (birefringence that does not disappear when the strain is removed). It is described by Bascom[16] as the "poor adhesion" case and is often observed when using untreated or high modulus carbon fibers. The second mode has high ISS values, short to almost no crack propagation distances, and bright birefringence patterns with regions of plastic deformation along the interface. It corresponds to "good adhesion" and is generally observed when using commercially-treated fibers of high strength or intermediate modulus. In the third mode, a matrix crack normal to the fiber at the fiber break propagates rather than the interfacial crack. This generally occurs with good interfacial adhesion and either a low modulus, high strain matrix resin or a stiff, brittle matrix resin.

Recently Piggott described the micromechanics of many different failure modes.[17] The poor adhesion case is well characterized by the friction factor approach for the debonded region coupled with the assumptions of perfect bonding and elastic behaviour for the bonded portion of the fragment. The matrix crack mode was

recently modelled by Gent *et al.* and results when the matrix fracture energy is less than the interfacial fracture energy provided geometrical constraints are considered.[18] The good adhesion interfacial crack mode is the most common and is also the most desired in terms of composite properties. When a fiber fails, energy is absorbed in the plastic deformation occurring with interfacial crack propagation. This case has been the most difficult to model convincingly though many approaches have been taken.

Work by Galiotis *et al.*,[19,20] using laser Raman spectroscopy to measure the fiber strain during a fragmentation test, has confirmed behaviour closely resembling elastic (shear-lag) behavior around embedded short fibers before fragmentation. At high strains after fragmentation for an untreated carbon fiber/epoxy system, results consistent with frictional slipping were observed. After fragmentation for a treated carbon fiber/epoxy system, fiber strains were observed consistent with debonding on the fragment ends and a well bonded central region, but the fiber strain build-up in the loading regions are not consistent with any simple model.

In addition to the micromechanics models which include elastic, plastic, frictional slipping, and brittle crack propagation behaviour, the chemistry of the interface must also be considered. Drzal has shown that the ISS increases with oxygen concentration of the fiber surface[4]. In these systems the neat resin and fiber mechanical properties remain constant, indicating the need to introduce chemistry into models for the fragmentation test. Schultz *et al.* show a correlation between fragmentation results and acid-base or acceptor donor capabilities of fiber surfaces as measured by inverse gas chromatography.[21] Snow *et al.* use the energy of complex formation between resin model compounds and hydrogen bond acceptor and donor probe molecules to measure relative donor-acceptor strengths of thermoset monomers and cured resin model compounds.[22] A correlation was noted between hydrogen bond acceptor strength and adhesion as measured by the fragmentation method. The technique was also used to show that in a mixture of partially cured thermoset in monomer, in some cases preferential adsorption of either products or reactants on the fiber surface would be expected, and in some cases neither component should favourably adsorb. It has long been speculated that factors such as preferential adsorption and relative diffusion of reactants can perturb stoichiometry and result in a gradient of properties near the interface.[4]

A correlation of interfacial chemistry with fragmentation results is difficult when there is not a proper means to correct for either bulk or interfacial property changes. It is difficult to evaluate models of fragmentation behavior when desired bulk property changes result in undesired interfacial chemistry or property changes. In this work we study mechanical property influences on the fragmentation test by physically aging the thermoset single fiber composites to alter mechanical properties without changing interfacial chemistry.

3. EXPERIMENTAL

3.1 Sample Preparation

The matrix resin was DGEBA-based epoxy, Epon® 828, (Shell Chemical), cured with metaphenylenediamine (mPDA). The resin was selected primarily because the failure

strain was greater than 6% (which is more strain than required for the fragmentation test and leaves room for embrittlement), the glass transition is low enough so that samples can be annealed near T_g without degradation, and there is a fragmentation database for this resin in the literature. A single batch of Epon 828 was used. The mPDA was obtained from Aldrich and was purified by distillation at 170°C and 6 torr. The fibers were unsized Hercules AS4 fibers and were used as received. The resin was prepared by degassing the Epon 828 at 70°C on a rotary evaporator, adding 14.5 phr mPDA and degassing 1 minute beyond the dissolution of the amine. The epoxy was then poured into a mold preheated to 75°C. The cure cycle was 2 hrs at 75°C, 1 hr at 125°C, and 0.5 hr at 185°C. Heating the cooling rates were 2° C/min. Cured panels were stored under desiccant.

Samples with and without fibers were made as roughly 6.5 × 6.5 × 0.125 inch (16.5 × 16.5 × 0.32 cm) plates in an aluminium mold coated with a dry fluorocarbon release agent. The mold consisted of two 3/8-inch (0.95 cm) polished aluminum plates separated by 1/8 inch (0.32 cm) thick brass U-shaped gasket. The mold was placed vertically in the oven and filled through the top of the U. The fluorocarbon release agent (MS-122, Miller-Stevenson) was sprayed on the polished surfaces before mold assembly and, after drying, the surfaces were wiped with a lint-free cloth. The release agent did not affect the fragmentation results as compared with samples without release agent in silicone molds. Fibers were mounted across a square frame of 1/16 inch-(0.16 cm) thick aluminum with spacers to insure the fibers were in the center of the 1/8-inch (0.32 cm) thick resin panel. Fibers were secured on the frame with double-stick tape and 5-minute epoxy. No effort was made to control fiber pre-load though consistent fragmentation *versus* strain profiles were obtained during testing. Samples for the various tests were cut using a Tensilkut router with carbide bits. ASTM D638 type I specimens were machined for tensile tests, ASTM D695 specimens for compressive loading, and ASTM E8 subsize specimens with 1-inch (2.5 cm) gauge lengths for critical length testing.

3.2 Thermal Treatment and Characterization

The above curve cycle was developed to force the epoxy to full conversion. Subsequent thermal treatments did not appreciably advance the glass transition nor show noticeable oxidation by IR spectroscopy. To maximise the range of properties obtained by altering the thermal history, samples were rapidly quenched as well as physically aged close to the glass transition temperature. Residual stresses were minimized during quenching by surrounding the epoxy panel with 3/16-inch (0.45 cm) of Teflon and 1/4- inch (0.64 cm) aluminum. The temperature at the center of the panel was measured during quenching and it compared well with the infinite slab heat conduction boundary value solution of Carslaw and Jaeger.[23] According to this solution, during cooling the majority of the temperature gradient will occur in the Teflon and the center and surfaces of the epoxy plate should never be more than 12°C apart even though a quench rate of 40°C/min was obtained through the glass transition region.

All panels were quenched. Aged panels were subsequently heated under vacuum for 100 hours at either 135°C, 145°C or 152°C and then allowed to cool slowly. Physical

aging was followed by DSC and density measurements on the aged panels. Samples were taken from at least four regions of the panel and measurements were averaged. The glass transition temperature was taken as the midpoint of the transition as measured on heating at 10°C/min. Enthalpy relaxation was determined by subtracting the second DSC scan from the initial scan. This procedure results in a small area below T_g being subtracted from a larger endothermal peak to yield the net enthalpy recovery.[24] For these measurements scan rates of 20°C/min were used. Density was measured by a buoyancy technique using degassed distilled water (ASTM D792) and averaging values from 4 (roughly 1 gram) samples. Tensile measurements were carried out on an Instron 4206 testing machine. ASTM D638 type I specimens were used at 0.05 in/min crosshead displacement with a clamp-on extensometer to measure strain. Bonded strain gauges were used for Poisson's ratio measurement. ASTM D695 geometry was used for compression measurements. A clamp-on extensometer was used and the crosshead displacement was 0.05 in/min. At least four specimens were tested for each evaluation.

3.3 Fragmentation Test

Fragmentation results were obtained using a hand-operated straining device mounted on a polarizing light microscope. Strain was measured as displacement of grips by a digital displacement gauge. This relative strain does not include corrections for the dog-bone cross-section of the tensile coupon or for initial seating in the grips. Fragments were measured using a viewing tube and digitizing pad. The number of fragments was counted after every 0.1 mm displacement. At least 8 specimens were tested for each thermal history with roughly 500 fragments. The ISS was calculated from the Kelly and Tyson equation[7] (eq. (1)) estimating l_c as 4/3 times the mean fragment length. For this fiber/epoxy system, the Weibull and Gaussian means were equal. The fiber stress at l_c was estimated from the log-log extrapolation of tensile tests on single fibers at three gauge lengths. For this fiber, Hercules AS4, Weibull extrapolations from all three gauge lengths nearly coincided with each other and with the log-log extrapolation. Fiber diameters were measured with a laser diffraction technique ($d = 7.13 \pm 0.26\,\mu m$). Details of the fiber measurements are reported elsewhere.[14]

4. RESULTS

4.1. Physical Aging

The glass transition of the fully-cured epoxy is 166°C. Physical aging of the neat and fiber-containing panels was carried out for 100 hours under vacuum at 135, 140, and 152°C. The aging process resulted in a slight increases in the glass transition of about 2°C. The enthalpy relaxation associated with the physical aging process is shown in Table 1 and representative DSC traces are shown in Figure 1. From the DSC traces the enthalpy recovery peak is larger, sharper, and shifted to higher temperature for the AGE152 panel relative to the AGE135 and AGE142 panels. When the areas below the recovery endotherm peak, which are due to the inability of the aged resin to absorb energy, are subtracted from the recovery endotherms, the net enthalpy recovery is very

TABLE I
Physical Aging Characterization

Sample	ρ_q (g/cc)	ρ_a (g/cc)	ΔH (J/g)
QUENCH	1.2027 ± .0011	–	–
AGE135	1.2047 ± .0003	1.2045 ± .0007	1.44 ± .06
AGE140	1.2041 ± .0002	1.2048 ± .0007	1.42 ± .13
AGE152	1.2054 ± .0004	1.2054 ± .0004	1.35 ± .4

ρ_Q before aging (quenched), ρ_A after aging.

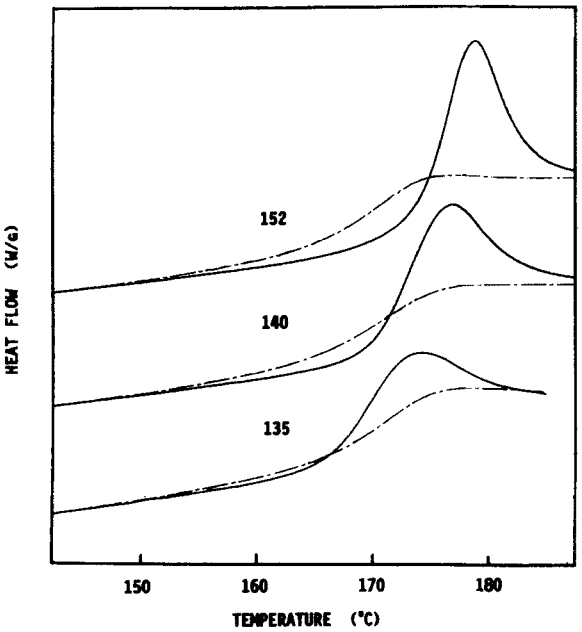

FIGURE 1 DSC scan after aging for 100 hours at specified temperature and immediate rescan. Substraction of the area below T_g from the endotherm above T_g gives net enthalpy relaxation. (Solid line is first scan, broken line is second scan)

similar for the three aging conditions. Standard deviations for these measurements were high. Possible sources of the scatter in the data are small baseline shifts which greatly affect the subaging peak area, random aging variations in the panels due to crosslink density or internal stress variations, and the small magnitude of the recovery endotherms.

The densities of the aged and quenched panels before and after aging are also shown in Table I. The densities after quenching but before aging are within 0.22% of each other which indicates consistency in the formulation and curing of the panels. Physical aging does not result in a measurable change in density within the precision of the measurements (0.07%).

4.2 Mechanical Properties

Mechanical property changes for the aged panels are summarized in Table II. In tension, the initial modulus and strength do not change significantly with aging, but the failure strain does, decreasing from 7.9% for the quenched resin to 5.3% for AGE135. In compression, the initial modulus does not change significantly with aging. Compressive failure could not be achieved due to sample size/fixture geometry constraints which forced stoppage of the measurement at about 9% strain. In a few experiments where the samples were capped with 1/16- inch (0.16 cm) aluminum to lengthen them, the range was extended to 15% strain, and compressive failure or a well-defined yield point still had not occurred. In both tension and compression, though the initial moduli for aged and quenched samples are about the same, the aged panels are significantly stiffer as shown in Figure 2. The secant modulus at 3% strain is 10% higher for the aged specimens in compression and 8% higher in tension. The increase in stiffness in compression is indicated in Table II as the stress observed at 9% strain. Though not formally studied, compression samples to 9% strain had little to no permanent set and there was a time dependency to the dimensional recovery indicating viscoelastic behavior. Preliminary stress relaxation experiments indicate a shift to longer relaxation times with aging. In Figure 2, a change from engineering to true stress to account for area changes during the experiment would bring the tension and compression curves closer together, but not eliminate the difference between them. Poisson's ratio did not measurably change with aging and there was roughly a 2% decrease in expansion coefficient with aging.

4.3 Fragmentation Test

The fragmentation results are summarized in Table III. There is no significant change in mean fragmentation length or calculated ISS with aging; however, there is a signifi-

TABLE II
Mechanical Properties

Tension Sample	Modulus (MPa)	Strength (MPa)	Failure strain
QUENCH	2970 ± 110	88.7 ± 1.3	7.9 ± 1.0
AGE135	2960 ± 70	85.8 ± 4.7	5.3 ± 0.9
AGE152	3030 ± 40	90.3 ± 4.1	5.7 ± 0.9

Compression Sample	Modulus (MPa)	Yield* (MPa)	Poisson's ratio**	Thermal expans. ($x10^{-6}$/°C)
QUENCH	3140 ± 90	137 ± 4	.36	70.2
AGE135	3050 ± 100	147 ± 8	.36	68.9
AGE152	3110 ± 90	147 ± 7	.37	68.7

* stress at 9% strain.
** at 1% strain.

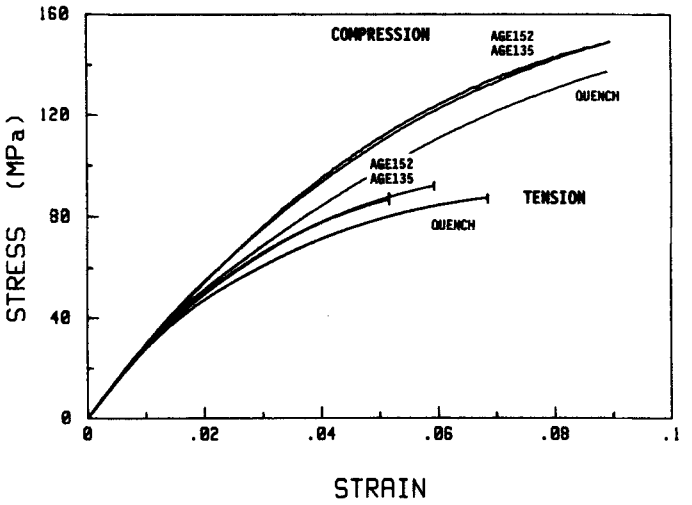

FIGURE 2 Engineering stress-strain response of aged and quenched samples in tension and compression. Compression tests were stopped at 9% strain.

TABLE III
Fragmentation Results

Sample	l (mm)	Number fragments	ISS (MPa)	1st Fragment strain
QUENCH	.48	715	32	.026
AGE135	.50	511	31	.034
AGE140	.47	522	33	.032
AGE152	.50	358	31	.034

cant change in relative strain at firs t break. First fragmentation events occur around 2.6% strain for the quenched specimens and 3.3% strain for the aged specimens. The fragmentation history versus strain is shown in Figure 3. In this figure, each curve represents a separate panel of roughly 8 test specimens and 500 fragmentation events. The aged and quenched panels form two groups of curves with the aged panels shifted to roughly 0.4% higher strain.

5. DISCUSSION

5.1 Physical Aging

The 2° C increase in glass transition temperature with annealing is probably due to a very small amount of additional crosslinking. This could be caused by reaction of residual isolated epoxy groups with hydroxyl groups or a reported fifth functionality of meta-phenylenediamine.[25] Expressions that relate the advancement in glass transition temperature to degree of crosslinking show a very sharp increase in T_g with slight additional crosslinking when the material is very highly crosslinked or near full

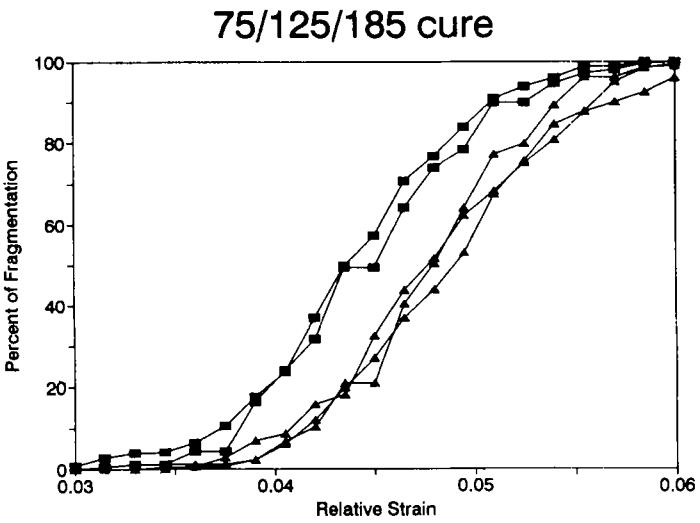

FIGUURE 3 Plot of normalized fragmentation *versus* strain for quenched and aged samples (squares for quenched panels, triangles for aged panels).

conversion.[26,27,28] The small increment in glass transition temperature should have little effect on mechanical properties considering that no change is seen in tensile properties for these two cure cycles: 75-125°C cure, $T^g = 146$°C[14]; 75–125–185°C cure, T_g 166°C.

The physical aging process was followed by measurement of enthalpy relaxation and density. The enthalpy recovery peaks observed in Figure 1 are sharper and at higher temperature for the higher annealing temperatures. This has been observed for many glasses and has been phenomenologically described by models based on the kinetics of the glass transition characterized by a broad nonexponential distribution of relaxation times.[29]

The enthalpy relaxation is roughly the same for the three annealing temperatures (Table I) indicating that the samples are physically aged to the same extent and that the rate of aging was not very temperature sensitive. The rate of aging depends both on the polymer segmental mobility (increases with temperature) and the deviation from equilibrium at the specified annealing temperature (which is usually greater at lower temperature). In general, the rate is low well below T_g, increases toward a maximum, and then decreases when just below T_g. The maximum is often in the 10 to 30C below T_g range. In this study, T_g-T_a = 14, 26, and 31°C. The data in Table I show a roughly constant rate of aging at the three different temperatures, indicating that there may be a broad maximum in the rate of physical aging *versus* temperature. A formal study of aging kinetics was not done but wide temperature ranges below T_g with roughly constant aging rates are seen in many systems,[30] including expoxies.[31] The roughly constant enthalpy recovery values also indicate that the systems have not been aged to equilibrium, because equilibrium values would be proportional to $T_g - T_a$.

No density changes were observed due to the physical aging process. In this study, samples for density measurement were removed from the panel before aging and

additional separate samples were removed after aging. Since the aging density changes were very small to nonexistent, sample variation or the precision of the method could preclude measurement of the actual density changes. The density change on aging is expected to decrease with crosslink density and stiffness of the backbone. Densification of less than the obtained standard deviations of 0.07% are not surprising, based on density changes of less than 0.05% for a similar epoxy reported in the literature.[32]

5.2 Mechanical Property Changes

Linear polymers generally show large changes in properties with physical aging. As chain mobility is reduced with crosslinks and stiffer backbone chains, the property changes with aging decrease. This is because the mobility of the rubbery material is reduced and the rubbery state becomes closer to the glassy state as is noted by smaller differences in the glassy and rubbery state heat capacities and expansion coefficients. The physical aging process results in a shifting of the relaxation spectrum to longer times. This results in an embrittlement of the materials. The results obtained for this system are comparable with other epoxies in the literature.[33–35] These include little to no initial modulus change with aging, reduced viscoelastic character, and an increase in compressive strength or yield stress. Though we did not reach a yield point in compression, the 7.3% increase in stress at 9% strain with aging can be used as an estimate of the magnitude of the yield stress increase with aging. This is very small compared with other measurements in the literature for epoxies aged for shorter times at similar $T_g - T_a$. This is believed to be the result of using a more rigid amine compared with other systems.

5.3 Fragmentation Results

Would the modest property changes be expected to affect the fragmentation results? This can be looked at on two levels, the simple elastic and plastic deformations discussed above or the more realistic models involving crack propagation. No significant change would be expected if the fragmentation test followed the shear-lag models because the aged and quenched specimens have roughly the same initial modulus and Poisson's ratio (and, therefore, shear modulus). If the adhesion measured by the fragmentation test was limited by the plastic deformation of the matrix, then the increase in shear yield strength due to aging should result in an increase in measured adhesion. An increase in shear yield strength has been shown to correlate with decreases in fracture energy for crack initiation in similar epoxies.[34,36] If this affects the interfacial crack growth in the fragmentation specimens, larger fragmentation lengths and decreased adhesion should be observed.

No change in fragmentation results was seen for the property changes incurred in this study. The physical aging conditions used to embrittle the epoxy were thought to be quite severe (100 hours just below T_g, probably at a maximum rate of aging) and other epoxy systems age to equilibrium in this time.[35] Slower aging rates in this epoxy system are probably related to the stiffer backbone and higher crosslink density as a result of the particular aromatic amine used. Since these samples were not physically aged to equilibrium, a definitive statement concerning the resistance of interfacial

adhesion to the effects of physical aging cannot be made. However, the smaller property changes noted in this case relative to other epoxies in the literature, with lower glass transition temperatures and aged at similar $T_g - T_a$, support the decreased importance of physical aging as crosslink density and T_g are increased.

The largest property changes induced by aging are the increase in stiffness at higher strains in tension and compression and the apparent increase in compressive yield stress indicated by the 7.3% increase measured at 9% strain. These changes are large enough so that one might expect a change in adhesion through either the crack-propagation mechanism or the shear-yielding mechanism discussed above. No change in fragmentation results was observed. Unfortunately, the property changes are small enough (considering the 6% variation in mean fragment length between AGE135, AGE152, and AGE140) that the lack of change in fragment lengths with aging cannot be used to discount the possibility of shear strength changes influencing the fragmentation process or to confirm the applicability of the shear-lag models. The successes of the approach are that modest property changes were induced by physical aging with no chemistry change at the interface and there was not a change in failure mode during fragmentation testing. Future attempts along these lines should use a thermoset matrix that shows greater property changes with aging, yet still exhibits the type of fragmentation behavior observed in practical matrix resins. Another possible reason for the lack of change in fragmentation lengths is that the interfacial region did not age like the bulk matrix. Though a stable T_g was reached in the matrix, hindered chain movements near the stiff fiber surface could have increased the effective glass transition, or preferential adsorption of the amine curing agent on the fiber surface could decrease the glass transition in the interface region below the annealing temperatures.[37] The possibility of preferential adsorption can be eliminated by using a one-component thermoset resin such as the cyanate ester resins. Regardless of what is done, there will always be the possibility of a gradient in properties emanating from the interface.

The increased strain necessary for fragmentation in the aged panels is difficult to explain. If carbon fibers are not prestressed when the panels are made, the difference in matrix and axial fiber expansion coefficients will normally put the carbon fiber in compression when the specimen is cooled from cure temperature. The increased strain required for the aged panels suggests that these fibers are initially in a higher state of compression. The changes in the neat resin with aging cannot account for this. There is little or no change in modulus, T_g, and Poisson's ratio. The two percent decrease observed in expansion coefficient of the aged panel would decrease the residual stresses in the carbon fiber, not increase them. The neat resin will contract roughly 1% when cooled from T_g to room temperature and so the roughly 0.4% strain difference in strain at fragmentation is difficult to explain. One possible explanation is that the epoxy gelled at 75°C on the 75-125-185°C cure cycle and established a zero stress state at this temperature which did not increase significantly during the remaining cure cycle. On aging for 100 hours near T_g the viscoelastic material could have relaxed and increased the zero stress temperature closer to the annealing temperature. Roughly a 40°C increase in zero stress state would account for the shift in fragementation strain.

6. CONCLUSIONS

An attempt was made to study mechanical property influences on the fragmentation test without any changes in chemical variables by physically aging the samples. The physical aging process produced small changes in mechanical properties consistent with embrittlement of the epoxy and a shifting of relaxation processes to longer times. No change was seen in initial modulus. The observed stiffening in compression was related to increased shear yield strength and expected fracture strength decreases. Based on these property changes, the shear-lag model is most consistent with the observed "no change" in interfacial adhesion by the fragmentation test. The small magnitude of the property changes precludes dismissing any fragmentation mechanism. The aged panels consistently fragmented at higher strains than the quenched panels. One possible explanation for this is the advancement of the zero-stress temperature with the long-term annealing treatments that were used to age the specimens physically. If this is indeed what happens, multi-dwell cure cycles to reduce residual stresses may only temporarily minimize the zero-stress temperature in composite parts.

Acknowledgement

The authors wish to acknowledge the Office of Naval Research for financial support.

References

1. M. J. Pitkethly, *et al.*, *Comp. Sci. Tech.*, **48**, 205 (1993).
2. L. T. Drazal, M. Madhukar, *J. Mat. Sci.*, **28**, 569 (1993).
3. L. T. Drzal, M. J. Rich, J. D. Camping, W. J. Park, in *Proceedings of the 35th Annual Technical Conference* (Reinforced Plastics/Composites Institute, The Society of the Plastics Industry, Inc), Section 20-C, 1 (1980).
4. L. T. Drzal, M. J. Rich, P. F. Lloyd, *J. Adhesion*, **16**, 1 (1982).
5. L. T. Drzal, M. J. Rich, M. F. Koenig, P. F. Lloyd, *J. Adhesion*, **16**, 133 (1983).
6. L. T. Drzal, M. J. Rich, M. F. Koenig, *J. Adhesion*, **18**, 49 (1985).
7. A. Kelly, W. R. Tyson, *J. Mech. Phys. Sol.*, **13**, 329 (1965).
8. R. B. Henstenburg, S. L. Phoenix, *Polym. Compos.*, **10**, 389 (1989).
9. B. Yavin, H. E. Gallis, J. Scherf. A. Eitan, H. D. Wagner, *Polym. Compos.*, **12**, 436 (1991).
10. A. N. Netravali, R. B. Henstenburg, S. L. Phoenix, P. Swartz, *Polym. Compos.*, **10**, 226 (1989).
11. J. M. Whitney, L. T. Drzal, **ASTM STP 937**, pp. 179–196 (1987).
12. H. L. Cox, *Brit. J. Appl. Phys.*, **3**, 72 (1952).
13. EL. M. Asloun, M. Nardin, J. Schultz, *J. Mat. Sci.*, **24**, 1835 (1989).
14. J. P. Armistead, A. W. Snow, *Polym. Compos.*, in press.
15. V. Rao, L. T. Drzal, *Polym. Compos.*, **12**, 48 (1991).
16. W. D. Bascom, R. M. Jensen, *J. Adhesion*,**19**, 219 (1986).
17. M. R. Piggott, in *Composite Applications: The Role of the Matrix, Fiber*, and *Interface*, T. Vigo and B. Kinzing, Eds. (VCH Publishers, Inc., New York, 1992), Chapt. 9.
18. A. N. Gent, Chi Wang, *J. Mat. Sci.*, **28**, 2494 (1993).
19. M. Melanitis, C. Galiotis, P. L. Tetlow, C. K. L. Davies, *J. Comp. Mat.*, **26**, 574 (1992).
20. C. Galiotis, *Comp. Sci. Tech.*, **48**, 15 (1993).
21. J. Schultz, L. Lavielle, C. Martin, *J. Adhesion*, **23**, 45 (1987).
22. A. W. Snow, J. P. Armistead, *J. Adhesion*, submitted
23. H. S. Carslaw, J. C. Jaeger, *Conduction of Heat in Solids*, (Oxford University Press, 1959), p. 200
24. M. J. Richardson, N. G. Savill, *Polymer*, **18**, 413 (1977).
25. J. C. Illman, *J. Appl. Polym. Sci.*, **10**, 1519 (1966).
26. A. Hale, C. W. Macosko, H. E. Bair, *Macromolecules*, **24**, 2610 (1991).
27. J. P. Pascult, R. J. J. Williams, *J. Poly. Sci. Phys.*, **28**, 85 (1990).

28. A. T. DiBenedetto, *J. Poly. Sci. Phys.*, **25**, 1949 (1987).
29. I. M. Hodge, A. R. Berens, *Macromolecules*, **15**, 762 (1982).
30. L. C. E. Struik, *Physical Aging in Amorphous Polymers and Other Materials* (Elsevier, New York, 1978).
31. R. A. Venditti, J. K. Gillham, *J. Appl. Polym. Sci.*, **45**, 1501 (1992).
32. K. P. Pang, J. K. Gillham, *J. Appl. Polym. Sci.*, **37**, 1969 (1989).
33. Z. H. Ophir, J. A. Emerson, G. L. Wilkes, *J. Appl. Phys.*, **49**, 5032 (1978).
34. A. -T. Truong, B. C. Ennis, *Polym. Eng. Sci.* **31**, 548 (1991).
35. C. G.' Sell, G. B. McKenna, *Polymer*, **33**, 2103 (1992).
36. U. M. Vakil, G. C. Martin, *J. Mat. Sci.*, **28**, 4442 (1993).
37. T. P. Skourlis, R. L. McCullough, *Comp. Sci. Tech.*, **49**, 363 (1993).